Design of a Solar Thermochemical Plant for Hydrogen Production

Ahmed, Qamar Rizwan
Chemical Engineering Department, NED University of Engineering & Technology, Karachi, Sindh, PAKISTAN

Mushtaq, Asim*[+]
Polymer and Petrochemical Engineering Department, NED University of Engineering & Technology, Karachi, Sindh, PAKISTAN

Ullah, Ahmed; Ali, Zaeem Uddin
Chemical Engineering Department, NED University of Engineering & Technology, Karachi, Sindh, PAKISTAN

ABSTRACT: *A plant was developed that uses a sulfur-ammonia thermochemical water-splitting process for H_2 production. Hydrogen is beneficial as a fuel in different industries and automobiles. Aspen Plus was used for the simulation of hydrogen plant modeling. This process consists of electrolytic oxidation of ammonium sulfite and the thermal breakdown of potassium pyro sulfate and SO_3 in the oxygen production half cycle. The reactions are carried out by solar thermal energy. The inlet stream is water, and the product streams are H_2 and O_2 gas. This research focuses on scrutinizing the economic strength of hydrogen production by electrolysis. During the research, it is clear that this type of study has great potential to reduce carbon emissions. That there is concluded economic potential for the electrolytic system. The model is for the full-scale operation that will produce approximately 1.3 lac kg H_2 / day. It is equal to 370MW. Design specifications were placed in strategic areas of this model to aid in its conversions. Model convergence is complex because of various material and energy recycle loops within the plant. The overall electricity needed to start the process is intramural from squandering heat. The thermal energy storage system will operate continuously without any shutdown. Three substitutes for hydrogen production from solar thermal energy have been inspected from both an efficiency and economic point of view. This observation shows that the possible alternative using solar energy with the help of thermochemical water splitting to manufacture H_2 is the best one. The other methods consider the direct conversion of solar energy into electrical energy by Si cells and H_2O analysis. The usage of solar energy to power a vapor cycle leads to the production of electrical energy.*

KEYWORDS: *Thermochemical, Hydrogen, Sulfur dioxide, Ammonia, Solar.*

INTRODUCTION

There are various political, social, and economic issues regarding the increasing need for electricity, accelerated consumption of fossil fuel, and environmental pollution, which requires highly resourceful and green energy

***** *To whom correspondence should be addressed.*
+ *E-mail: engrasimmushtaq@yahoo.com*
1021-9986/2023/2/508-523 16/$/6.06

conversion technologies. There are many areas of study on durable energy sources, including hydroelectric wind, geothermal, biomass, solar photovoltaic, and solar thermal, each having its benefits and loss. Moreover, fuel cells using hydrogen and other hydrocarbons with distinct properties of high efficiency and green process have attracted significant attention in the past few years. The current work is distinct on solar thermal energy storage, where the thermal energy from the sun is stored for hydrogen production [1, 2]. Light is the essential source of energy of the sun, and its change to chemical fuel has occurred on a Giga joule scale by photosynthesis for a long time. Harvesting sun-based light, the change of photon energy into a potential electrochemical results in the electrolytic transformation of water into oxygen and hydrogen [3, 4].

The main research objective is to determine the economic feasibility of hydrogen production from sulfur ammonia using solar thermal energy. The eventual research objective was to choose one or more ruthless concepts for the pilot-scale to abbreviate using highly intense solar energy. Pilot-scale plant production results would be used as the substructure for searching public and private expedients for full-scale plant production and testing.

Economic success in this progress would afford the public a sustainable and limitless source of energy carrier for use in electricity load-leveling C free shipment fuel. Hydrogen manufacture by thermochemical water breaking is a chemical procedure that fulfills the breakdown of water into H_2 and O_2. It utilizes only heat or an amalgamation of heat and electrolysis. Solar thermal hydrogen production also linkup these objectives through executing photoelectrolysis. The surface of optoelectronic is in contact with an electrolyte furnished by a photovoltaic cell. Numerous solutions are made due to the motive of comprehension of the general potential of H_2 manufacturing by electrolysis. Further studies are needed to be carried out for this objective. The literature survey studied thermochemical water splitting uses high temperature from intensive solar power or the misuse of thermonuclear power and reactions to produce H_2 and O_2 from H_2O. It is a deep routed technology channel, with potentially low or no greenhouse gas released. The thermochemical sulfur, ammonia water breaking procedure uses a high-temperature range from 500 to

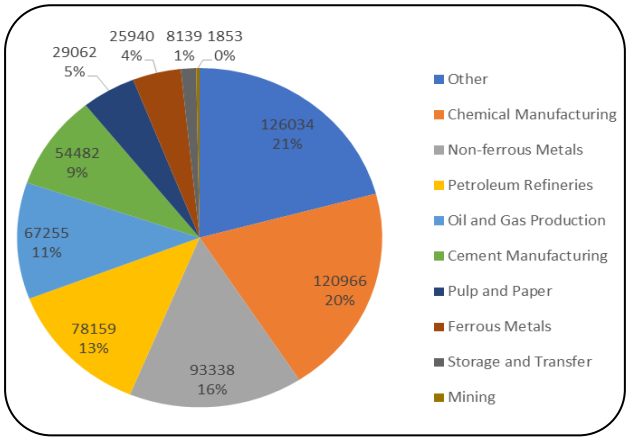

Fig. 1: SO_2 emission in different sectors.

2000 ˚C to precede a series of chemical reactions that produce H_2 gas. The chemicals utilized in the process are recycled within each loop. Several thermochemical water breaking cycles have been found for H_2 production, each with different operating order, engineering challenges, and hydrogen production chance. By far, solar and nuclear navigation produces a high-temperature thermochemical SA- cycle to produce H_2 with nearly zero greenhouse gas discharge using water and sunlight [4, 5]. NASA satellite data find out approximately 500 significant sources of SO_2 emission worldwide, including natural resources like volcanoes is shown in Fig. 1. Almost 60% of the current total emissions are due to organic evolution. Sectors including coal combustion, industries, power combustion, smelters, oil and gas refining contributed 31%, 10%, and 19%, respectively [6, 7].

Due to environmental pollution, the amount of sulfur dioxide exposed to air is continuously reducing. In the future, it will be further reduced as health can be badly affected and the environment would also be polluted. This solar thermochemical plant for hydrogen is also less hazardous as it does not expel out waste gases such as sulfur dioxide and ammonia but recycle them and utilize them for better economy and zero greenhouse gases emission [8, 9]. Ammonia has a great demand in the world. But ammonia can significantly affect both human health and the environment, as shown in Table 1. It causes adverse effects on bio-diversity with some species and habitats, especially receptive to ammonia pollution. About 90% of NH_3 produced is utilized in the fertilizer Industry. It has other uses, such as household cleaning products and other goods manufacturing. At the start of the 21st-century total NH_3 emission in the United Kingdom were calculated

Table 1: Consequences of ammonia.

NH_3 Concentration in Air (ppm)	Health Symptoms
<25	Detectable by smell
30	Difficulty in breathing
50	OSHA maximum exposure limit
100	Problems in eye, throat, and mucous membrane
140	It has no long-term effect in exposure for less than 2 hrs.
400	Damage mucous membrane for more than one-hour exposure.
500	Immediate danger to life.
1000	Hazardous to the airway.
1700	Deadly after short exposure in less than half an hour.
5000	Immediate hazard to life.
>15000	Complete body protection is necessary.

to be 283kt N per year with 228kt N per year from agriculture sources [10, 11]. Utilization of the ammonia emission through this research effectively mitigates the effect of polluted and toxic emissions.

Many firms produce green ammonia, a way to NH_3 in which H_2 gas is derived from the electrolysis of water followed by renewable energy sources. Mostly green ammonia will cost 2 to 4 times more conventional ammonia. According to a current report by IMF, Pakistan ranks third in the world among those countries facing difficulties because of a shortage of water. Research reports of United Nations Development and Pakistan Council for water resources also warn the authorities about the absolute water scarcity in the south Asian region by 2025. The water problem and its shortage have affected and will continuously affect the strength of communities. The overview of the worldwide water challenge shows many difficulties and flashpoints [12, 13]. Since hydrogen production water is the essential raw material and according to IMF Pakistan per capita yearly water availability is $1020m^3$. Back in 2009, Pakistan's water availability was about $1500m^3$. In the future, the water shortage problem will be resolved up to some extent if more water reservoirs shall be established in Pakistan.

Present, past, and future of product

H_2 and energy have a long shared history, composing the 1st internal combustion engines over almost 200 years before an essential part of the modern refining industries. The future of hydrogen provides a substantial and independent survey of H_2 gas. The method in which hydrogen can help get a clean, protected, and inexpensive

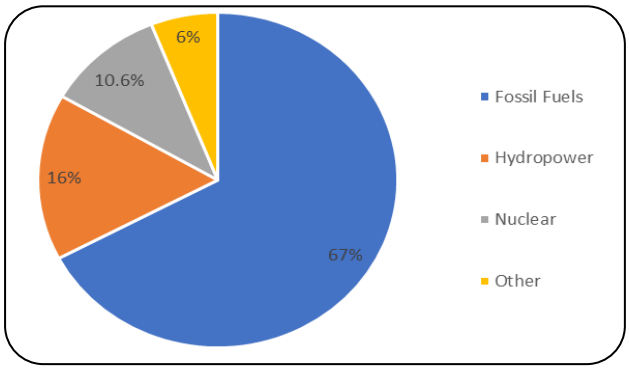

Fig. 2: Hydrogen production.

energy future. Since; the demand for hydrogen is increasing day by day in almost every sector, its production should also be enough to meet the required need for H_2 gas shown in Fig. 2 [14, 15].

The future of hydrogen is secured cost of hydrogen production from renewable energy would occur 30% by 2030 due to a decrement in renewables [16, 17]. Oxygen is the essential element on earth for aerobic organisms. It is observed that fossil fuel combustion is the most significant contributor to the present oxygen deficit. The dead zone has appeared compared to the simultaneous increase of CO_2 and its effects on the atmosphere; the reducing climatic O_2 is far beyond the focus of the research area [18]. The need for high-grade O_2 gas in industries is overgrowing. The market has established air separation units, especially in developed countries with local producers. However, industrial oxygen uses a large amount of electricity, and outstanding equipment is required to separate and store it, which represents a problem to the steady cash flow of the market [19, 20].

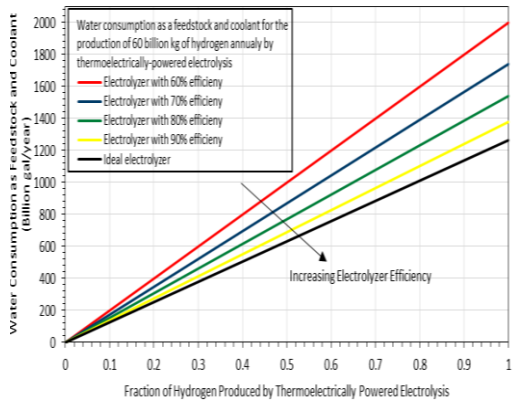

Fig. 3. Hydrogen production by electrolysis

However, there are various methods of producing hydrogen. Steam reforming transforms (CH_4) methane and other hydrocarbons in marsh gas into H_2 and CO by reacting with steam in the presence of Ni as a catalyst. Steam electrolysis uses heat energy in electrical energy to provide some energy needed to break down water making the process more efficacious [21, 22]. Thermochemical water splitting uses different chemicals and heat in various steps to break down water into H_2 and O_2. Fig. 3 shows the hydrogen production by electrolysis. Photoelectrochemical type of system uses semiconductors like the photovoltaic cell to split water using only solar energy. Photobiological system microorganisms are used to split H_2O using solar energy. Bacteria and other biological organisms are used to split a biodegradable oxygen demand of biomass (BOD_5) into H_2 gas. Thermal water splitting utilizes a bulk temperature of nearly about 1000°C to split water. Gasification uses heat to split biomass or coal into natural gas from which hydrogen can be produced [23-25].

EXPERIMENTAL SECTION

Process selection

It has selected the solar sulfur ammonia thermochemical water-splitting process for hydrogen production because it is the most efficient overall process, which produces 1E5 Kg hydrogen per day with zero greenhouse gas emission. In this process, the raw materials are the cheapest and readily available. The chemistry of raw materials is significantly more accessible and understandable. No waste is produced during this process; another benefit is that the sub-product oxygen gas is made. Another factor while designing any plant or selecting any method is the process cost. The chosen process to produce hydrogen gas is the cheapest [26-30].

$$2NH_3\,(g) + SO_2\,(g) + H_2O\,(aq) - - - -\rightarrow \quad (1)$$
$$(NH_4)2SO_3\,(aq) \qquad (1 - \text{Chemical absorption})$$

$$(NH_4)2SO_3\,(aq) + H_2O\,(aq) - - - --> \quad (2)$$
$$(NH_4)2SO_4\,(aq) + H_2\,(g) \quad (2 - \text{Electrolytic oxidation})$$

$$(NH_4)2SO_4\,(aq) + K_2SO_4\,(l) - - - -> \quad (3)$$
$$2NH_3\,(g) + K_2S_2O_7\,(l) + H_2O\,(aq)$$
$$(3 - \text{Adiabatic mixing})$$

$$K_2S_2O_7\,(l) - - - --> SO_3\,(g) + K_2SO_4(l) \quad (4)$$
$$(4 - \text{Stored energy})$$

$$SO_3\,(g) - - - --> SO_2\,(g) + 1/2O_2\,(g) \quad (5)$$
$$(5 - \text{Electric heat})$$

The overall cyclic reaction means by reactions 1-5 is the splitting of water to produce H_2 and O_2 gas. The electrolytic oxidation of $(NH_4)_2SO_3$ occurs above the atmospheric temperature at moderately low pressures to produce hydrogen gas. Reactions third and fourth are forming a sub- through which (K_2SO_4) is reacted with $(NH_4)_2SO_4$ to form $K_2S_2O_7$ in the low temperature reactor. Potassium pyro sulfate is then added to the mild temperature reactor, where it is broken down to sulfur trioxide and potassium sulfate, closing the sub-cycle. The K_2SO_4 and $K_2S_2O_7$ form a miscible liquid melt which eases the severance and motion of chemicals in reactions third and forth in step five [31-32]. The manufacturing of O_2 occurs at high temperatures in the presence of activators or catalysts. Separation of O_2 from SO_2 happens when sulfur dioxide is absorbed in H_2O in reaction 1. No gas or liquid occurs in this process; all the reactions explained below have been signified in the laboratory through experiment without unexpected side reactions. By using the sub-cycle handling problem of the material can be minimized, melted or molten salt depository could be used as it well explained, and the solar thermal energy regaining could be working, concluding in simpler operating conditions. The modeling of the chemical plant is based on aspen Plus, and the designed and assessment of the solar area will be explained. The Aspen Plus model was a chemical plant to produce 1.7E5 kg per day of H_2 gas. But this is a vast plant; the system minimized to a more excusable unit size 25 MW maximum input power with average hydrogen manufacturing that is 5000kg per day. This system will be duplicated to meet the Design of the Experiment (DOE)

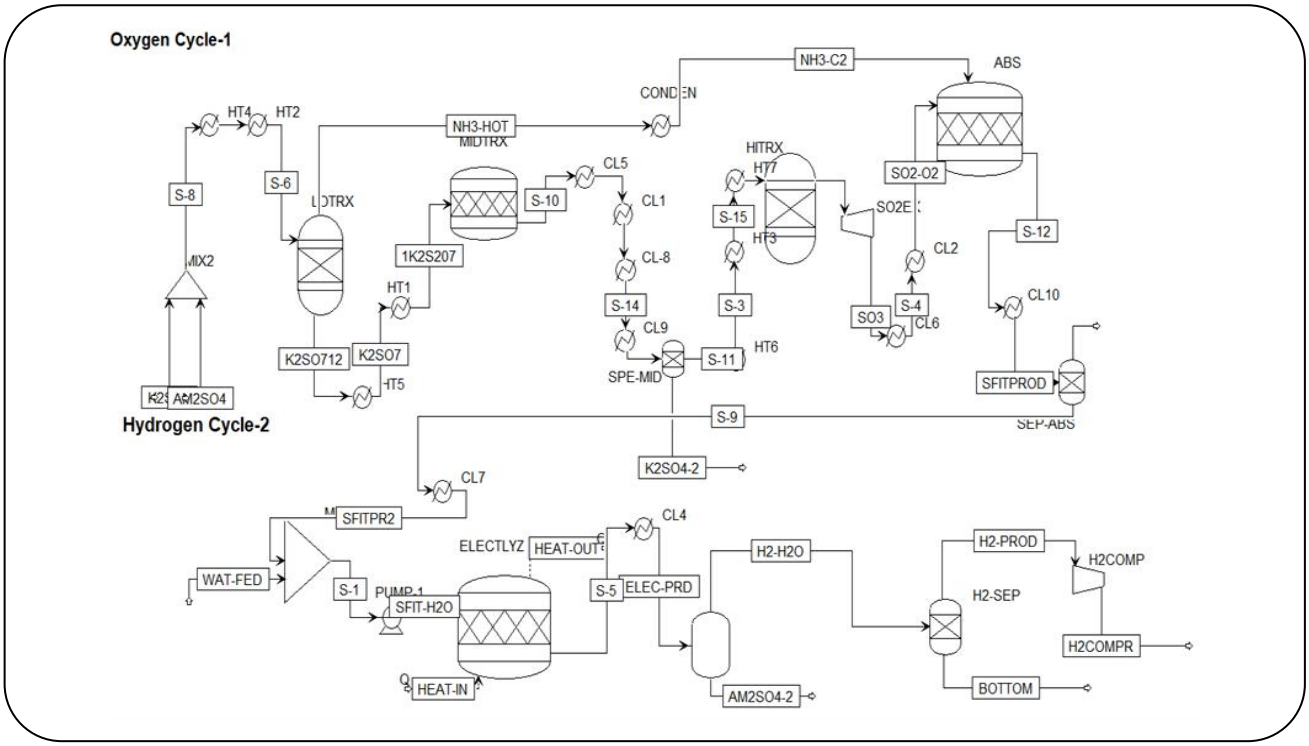

Fig. 4: Process flow of oxygen and hydrogen cycle.

target of 1E5 kg per day. Fig. 4 shows the process flow of the oxygen and hydrogen cycle.

Solar energy comes entirely from a solar storage system utilizing a phase change; the NaCl storage path allows the unstoppable operation of the process. This energy is fed to the mild temperature reactor for decomposing potassium pyro sulfate. The low temperature reactor works adiabatically on sensible heat of the inlet (reactant). The chemical absorber produces sufficient heat to keep its temperature according to the desired range. The electrolyzer operates on electrical energy that comes from the energy recovery system. The electric heating of a high-temperature reactor permits the solar storage system to work at low temperatures, increasing its proficiency and optimizing the system's energy balance. For the reactor volume, kinetic factor and $F_{AO}X_A$ are calculated by the given equation,

$$\text{Kinetic factor} = kT^n \quad (6)$$

$$F_{A0}X_A = (-r)_A V \quad (7)$$

Components selection

The thermochemical process for hydrogen production consists of a particular set of chemical reactions, including the thermal decomposition of molten potassium pyro sulfate ($K_2S_2O_7$) and gaseous sulfur trioxide (SO_3) in the oxygen production (half-cycle). Also, the electrolytic oxidation of aqueous ammonium sulfate in the hydrogen production (half-cycle). Table 2 shows the components are conventional, but some components in Aspen Plus® have some lacking towards the thermodynamic region, especially the ionic salts and electrolytes; higher temperature and melting of salt causes Aspen Plus® to calculate incorrect enthalpies. The component chemistry is defined for some components lacking thermodynamic data.

Electrolytes are essential in this work; potassium and ammonium salts are present. It is necessary to define the electrolyte chemistry; the electrolyte wizard has used the location of the electrolyte wizard, as shown in Table 3.

Property method selection

The thermodynamic model chosen for the equilibrium relations is ELECNRTL. It uses an unsymmetrical electrolyte NTRL model for ionic components' liquid phase states. Also, Henry's law for the supercritical state uses the Redlich-Kwong equation. It is used because the property bank of Aspen Plus does not contain parameters related to a component used. The oxygen half-cycle

Table 2: List of Aspen Plus® components.

Component ID	Component Type	Component Name	Alias
H_2O	Conventional	Water	H_2O
AM_2SO_3		Ammonium sulfite	$(NH_4)_2SO_3$
AM_2SO_4		Ammonium sulfate	$(NH_4)_2SO_4$
K_2SO_4		Potassium sulfate	K_2SO_4
$K_2S_2O_7$		Potassium pyro sulfate	$K_2S_2O_7$
NH_3		Ammonia	H_3N
SO_3		Sulfur trioxide	SO_3
SO_2		Sulfur dioxide	SO_2
O_2		Oxygen	O_2
H_2SO_4		Sulfuric acid	H_2SO_4
H_2		Hydrogen	H_2

Table 3: Generated electrolytes using Aspen Plus® electrolytes wizard.

Component ID	Component Type	Component Name	Alias
NH_4^+	Conventional	NH_4^+	NH_4^+
H_3O^+		H_3O^+	H_3O^+
K^+		K^+	K^+
HSO_3^-		HSO_3^-	HSO_3^-
OH^-		OH^-	OH^-
HSO_4^-		HSO_4^-	HSO_4^-
SO_3^-		SO_3^-	SO_3^{-2}
SO_4^-		SO_4^-	SO_4^{-2}

of the current work involves very high-temperature liquid potassium sulfate and potassium pyro sulfate salts. It will cause the decomposition of potassium pyro sulfate to potassium sulfate and sulfur trioxide. Simulation of these salt in Aspen Plus® is challenging because of the thermodynamics data regarding potassium and ammonium salt and their solid and liquid state [33-35].

Block method selection

The process requires theoretically simulated reactors, including Gibbs and stoichiometric reactors; the flow sheet includes many material heat and information flows. The Gibbs reactor is an equilibrium reactor that performs chemical and phase equilibrium calculations by Gibbs energy minimization. For this information and more on Gibbs reactors in Aspen Plus®, use help and search "Gibbs reactor." This reactor was chosen for reactions in low and high-temperature reactors because of chemical and phase equilibrium calculations. It requires the input of two operating conditions; pressure and temperature or heat duty. The user can also define the maximum number of fluid phases. Reactor Gibbs allows products to be explained to appear in particular phases. The low temperature reactor was used to simulate potassium pyro sulphate and ammonia; the low temperature reactor was labeled LOTRX. Gibbs reactor was used because the reactor is capable of calculating phase equilibrium for the vapor-liquid system; also, the kinetics of the system is not known by Aspen Plus®. The high-temperature reactor was used to simulate the high-temperature decomposition of sulfur trioxide. The high-temperature reactor was labeled HITRX Gibbs is also chosen to simulate this reactor because the reaction kinetics was not available in Aspen Plus®.

The stoichiometric block models were used in a reactor with specified reaction with conversion property. The reactor was chosen for the reactions simulated by the mid-temperature, chemical absorber, and electrolyzer. Still, the conversion of potassium pyro sulfate needed to be calculated by a design specification block for the chemical absorber because it was preferable to achieve

100% conversion of the ammonia and electrolyzer. After all, laboratory data on the transformation within the reactor were available. The mid-temperature reactor was used to simulate the decomposition of potassium pyro sulfate. The mid-temperature reactor was labeled as MIDTRX. RStoich was chosen for simulation because phase equilibrium data between liquid $K_2S_2O_7$ and K_2SO_4 and gaseous SO_3 were known. Heat exchanging equipment is being used to increase and decrease energy for the reaction to complete, especially for LOTRX, MIDTRX, and HITRX, as reactors are energy sensitive. Some of them are working on high temperatures unusually high. Furnaces are used as a heater are not working on the temperature exceeding 500 °C as operating temperatures are 800 ºC and 1000 °C.

Assumptions

Some assumptions to make the simulation a bit less painful include; limited number and reactor efficiency of side reactions, no change in the material stream, use of Gibbs reactor, un-symmetric electrolytes, efficient heater and coolers, the pure substance in the stream.

RESULTS AND DISCUSSION

For the most part, all parameters are calculated from Aspen Plus; the energy balance and heat integration are done through the help Aspen energy analyzer. As generating more heat than process requires, this excessive will be utilized. In this process itself, furnaces are also used for high-temperature requirements.

Material and energy balance

After running the simulation, significant errors were removed, and the overall product was achieved; several errors were present, but thanks to Aspen Plus's friendly user interface, they were released. The typical error was due to mole, but after converting it into mass balance, the error was significantly reduced; the cause of molar flow error is unknown [18-20].

Rate of accumulation (mass flow) = (8)
Mass flow rate into the system – Mass flow out of the system

Rate of accumulation (energy rate) = (9)
Energy rate into the system – Energy out of the system

It has a continuous system in mass flow and energy rate, so the accumulation rate is "0". Due to some calculation complexities, Aspen tends to generate minor irregularities in molar balance, but overall mass balance is appreciably shown in Table 4. Due to the system's complexity, major equipment of energy balances is included along with their demand overall flow sheet balance shown in Table 4.

Electrolyzer (ELECTLYZ Model Rstoic) is a stoichiometric reactor having the material and energy balance; the reactor is a reverse fuel cell handling the pressure of 9 bars and temperature of 130ºC. The stream, when entering into the reactor, is pre-cooled till 130.8ºC, giving enough energy, also increasing the overall efficiency and product quality. Material and energy balance for modeled electrolyzer reactor is shown in Table 5. Table 6 shows the vapor-liquid phase equilibrium and specific reaction rate constant in the electrolyzer reactor used in this study.

LOTRX Model RGibbs in low temperature reactor is chosen to Gibbs reactor, due to lack of reaction information, the reactor is pressure vessel handling pressure up to 9 bar and 400ºC. MIDTRX is a stoichiometric reactor having a material and energy balance; the reactor is a pressure vessel handling the pressure of 9 bar and a temperature of 834.5ºC. The stream, when entering into the reactor, is pre-heated till 800ºC, giving enough energy, also increasing the overall efficiency and product quality, as shown in Table 5. Table 6 shows the phase data for the mid-temperature MIDTRX reactor. HITRX or high-temperature reactor is classified as Gibbs reactor, having 1000ºC and 9 bar pressure, of the material and energy balance shown in Table 5. ABSRX is an absorber reactor; it is classified as a stoichiometric reactor; the operating temperature and pressure are 120ºC and 9 bar. This vessel works as the absorber and the reactor. Table 7 shows the heat integration summary of the Aspen Plus analyzer for the model used in this study.

Table 8 shows the summary of Aspen Plus analyzer heat exchangers (coolers).

Table 9 shows the terminal temperatures of entering and leaving a stream of the heat exchangers (heater) used in the designed Aspen model.

Agitated reactor

Agitated reactors are chosen because of their ability to use agitation to meet better mixing, high conversion, and better cooling; they are well suited for requirements, especially for best heat transfer. These reactors are the leading

Table 4: Overall flow sheet balance.

Conventional Components (kmol/hr)	In	Out	Generation	Relative Error
H_2O	185.901	167.489	-18.4128	0.00000
$(NH_4)_2SO_3$	1.07843	1.02593	-0.524931E-01	0.411218E-15
$(NH_4)_2SO_4$	20.5202	19.4927	-1.02744	0.173133E-15
K_2SO_4	30.0000	35.1606	5.16061	0.173133E-15
$K_2S_2O_7$	120.000	114.839	-5.16061	-0.118424E-15
NH_3	0.00000	2.15986	2.15986	0.205610E-15
SO_3	0.00000	4.76188	4.76188	0.186518E-15
SO_2	0.00000	1.47866	1.47866	0.00000
O_2	0.00000	10.4595	10.4595	0.00000
H_2SO_4	0.00000	0.00000	0.00000	0.00000
H_2	0.00000	19.4927	19.4927	0.00000
Total Mass Balance (kg/hr)	41932.6	41932.6	-	0.00000
Total Energy Balance (cal/hr)	-0.239497E+08	-0.239497E+08	-	-0.191939E-01

Table 5: Total balance for reactor .

Total Balance	In	Out	Relative difference
ELECTLYZ Model Rstoic			
Mass (Kg/hr)	6264.3535	6264.3535	0
Enthalpy (cal/sec)	-4790423.66	-4790423.66	-1.94413405E-16
LOTRX Model RGibbs			
Mass (Kg/hr)	41797.48	41797.48	-4.35191138E-15
Enthalpy (cal/sec)	-22141031.8	-22443661.4	0.0134839695
MIDTRX Model Rstoic			
Mass (Kg/hr)	37389.6	37389.6	0
Enthalpy (cal/sec)	-20302778.7	-23326572.4	0.129
HITRX Model RGibbs			
Mass (Kg/hr)	4115.60724	4115.60724	2.20986758E-15
Enthalpy (cal/sec)	-1141249.84	-849925.522	-0.255267783
ABSRX Model Rstoic			
Mass (Kg/hr)	12943.5843	12943.5843	-1.40532125E-16
Enthalpy (cal/sec)	-9088271.35	-9330161.6	0.0259256229

Table 6: Phase data for reactor.

Component	F	X	Y	K
ELECTLYZ Model Rstoic				
H_2O	0.776100171	0.859136332	0.234284936	0.272698205
AM_2SO_3	0.00474629148	0.00547368671	5.4426302E-95	9.94326217E-93
AM_2SO_4	0.0901795381	0.104000048	7.17289738E-95	6.89701356E-94
NH_3	0.00999219258	0.00801139414	0.0229170047	2.8605514
SO_3	0.0220172694	0.015556616	0.0641733663	4.12514947
SO_2	0.00678499909	0.00782182761	1.96394379E-05	0.00251085026
H_2	0.0901795381	9.610059E-08	0.678605054	7061403.62
MIDTRX Model Rstoic				
K_2SO_4	0.200071849	0.234308941	1.05383396E-79	4.49762591E-79
$K_2S_2O_7$	0.653796476	0.765676733	9.09789093E-79	1.18821567E-78
SO_3	0.146131675	1.43260703E-05	1.00	69802.8125
ABSRX Model Rstoic				
H_2O	0.820152291	0.871030595	0.168725029	0.19370735
AM_2SO_3	0.0937614596	0.101084494	2.93697911E-110	2.90546947E-109
NH_3	0.00986962733	0.000238201108	0.1331869	559.099906
SO_3	0.0217472033	0.0186995098	0.0607687608	3.24975166
SO_2	0.0067017736	0.00722481772	4.90711075E-06	0.000679201509
O_2	0.0477676447	0.00172238283	0.637314403	370.019036

Table 7: Aspen Plus analyzer heat integration.

Utilities	Actual	Target	Available Savings	% of Actual
Total utilities [cal/sec]	1.266E+07	7.301E+06	5.357E6	42.33
Heating utilities [cal/sec]	1.988E+06	6.554E+04	1.922E+06	96.70
Cooling utilities [cal/sec]	1.067E+07	7.235E+06	3.435E+06	32.20
Carbon emissions [kg/hr]	1.066E+04	6149	4515	42.34

Table 8: Aspen Plus analyzer heat exchangers (coolers).

Heat Exchanger	Hot temperature [°C]		Cold Temperature [°C]		Cold Side Fluid
	Inlet	Outlet	Inlet	Outlet	
ABS_heat_Exchanger	200.0	150.0	124.0	125.0	LP steam generation
ELEC-FLS_heat_Exchanger	75.0	25.0	-25.0	-24.0	Refrigerant 1
HEAT-OUT_Exchanger	132.9	130.0	30.0	35.0	Air
CL9	196.9	50.0			
CL10	150.0	50.0			
CL4	130.0	75.0			
MIDTRX_heat_Exchanger	834.5	834.0	249.0	250.0	HP steam generation
CL1	684.5	400.0			
CL5	834.5	684.5			
CL2	595.2	400.0			
CONDEN	400.0	200.0	174.0	175.0	MP steam generation
CL-8		196.9			

Table 9: Aspen Plus heat exchangers (heaters).

Heat Exchanger	Hot Temperature [°C]		Cold Temperature [°C]		Hot Side Fluid
	Inlet	Outlet	Inlet	Outlet	
HT2	1000.0	400.0	222.5	300.0	Fired heat (1000 °C)
HT4	250.0	249.0	28.1	222.5	HP steam
HT9	175.0	174.0	50.0	135.0	MP Steam
LOTRX_heat_Exchanger	1000.0	400.0	300.0	400.0	Fired heat (1000 °C)
HT6	250.0	249.0	50.0	196.8	HP steam
HT7	3000.0	2999.0	196.8	850.0	Very high temperature
HITRX_heat_Exchanger	3000.0	2999.0	850.0	1000.0	Very high temperature

Table 10: Detail sizing of agitated reactors.

Equipment	MIDTRX	ELECTLYZ	LOTRX
Liquid volume (L)	889.60	7881.342	889.60
Vessel diameter (meter)	0.6096	1.3716	0.6096
Vessel tangent to tangent height (meter)	3.048	5.334	3.048
Design gauge pressure (barg)	9.7105	9.7105	9.7105
Design temperature (°C)	889.6048	7881.34245	889.6048
Operating temperature (°C)	0.6096	1.3716	0.6096
Jacket design gauge pressure (barg)	3.048	5.334	3.048

equipment of the process LOTRX (low temperature reactor), MIDTRX (mid-temperature reactor), HITRX (high-temperature reactor). A design based on the parameters; volume handle, vessel diameter, and handle pressure are shown in Table 10.

Gas compressor

Compressors are mechanical devices, which increase pressure by reducing the volume; the purpose of the compressor is used to transport fluid in a pressurized vessel. The centrifugal gas pump is used, handling the pressure of 9 bars at temperatures of 25°C. Gas compressor the sizing is based on motor-based, the sizing parameters include; gas flow, design pressure, outlet temperature, and compressibility factor are shown in Table 11 [32-35].

Vertical vessels

Aspen Plus has divided the equipment separation; all equipment is phase separators. The design calculation for SPE-MID, the parameters are calculated as, L_s= 270.3 Ft, SR=9.1, D= 26.0 inch. Those include; mid-temperature reactor separator, electrolyzer flash, and hydrogen separator are shown in Table 12.

TEMA heat exchanger

Heat exchangers are energy exchanging equipment used for utilizing the energy of the fluid either by heating or cooling; the mixing prevented using solid material between the fluids. Heat exchangers are generally manufactured on ASTM or TEMA standards. The last piece of equipment to be designed is heat exchangers; here, TEMA standards are shown in Table 13.

Box furnaces

For reaching higher temperatures, furnaces are used; the utility requirements are liquid and gas fuels. The primary purpose of these furnaces is to get higher temperatures because heat exchangers don't do that. Box type Furnaces are chosen for their simplistic design, and high heat capacity are shown in Table 14.

Jacketed horizontal drums

Higher temperature reaction vessels are chosen to be drums because the reaction is sensitive to temperature and pressure. Both MIDTRX (mid-temperature reactor) and HITRX (high-temperature reactor) are designed to be jacketed horizontal drums are shown in Table 15.

Table 11: Equipment design gas compressors.

Equipment	H_2COMP2
Actual gas flow rate inlet (l/min)	2253.42150462
Design gauge pressure inlet (bar)	7.986
Design temperature inlet (°C)	100
Design temperature outlet (°C)	226.246
Design gauge pressure outlet (bar)	20.686
Driver type	Motor
Driver power (kW)	19.853
Molecular weight	2.01588
Specific heat ratio	1.415958
Compressibility factor inlet	1.00549
Compressibility factor outlet	1.010139

Table 12: Detail equipment design vertical vessels.

Equipment	SPE-MID	H_2-SEP	SEP-ABS	ELEC-FLS
Liquid volume (L)	2401.93	2401.93	3269.29	3269.29
Vessel diameter (meter)	0.9144	0.9144	1.0668	1.0668
Vessel height (meter)	3.6576	3.6576	3.6576	3.6576
Design gauge pressure (bar)	9.710	9.710	9.710	9.710
Design temperature (°C)	2401.93	2401.93	3269.29	3269.296
Operating temperature (°C)	121.11	121.11	177.7	121.11

Table 13: Detail design of heat exchangers.

Equipment	CL10	CL1	CL7	CL5	CL2	CL9	CL4	HT4	CL6	CONDEN	CL-8	HT6
Heat transfer area [sq.m]	91.26	1.04	759.01	1.62	1.94	48.59	42.78	0.72	2.69	1.87	13.19	1.87
Front end TEMA symbol	B											
Shell TEMA symbol	E											
Rear-end TEMA symbol	M											
Tube design gauge pressure [bar]	6.13	6.13	7.60	6.13	4.15	6.1358	6.135	30.014	4.15	6.135	6.137	30.014
Tube design temperature [°C]	177.7	627.7	192.11	862.27	627.7	227.77	157.77	257	877.58	427.7	427.77	257
Tube operating temperature [°C]	35	35	164.33	35	35	35	35	229.22	35	35	35	229.2
Tube outside diameter [meter]	0.0254											
Shell design gauge pressure [bar]	9.7104	9.7104	9.7104	9.7104	4.2104	9.7104	9.7104	19.6717	4.210	9.7104	9.7104	19.671
Shell design temperature [°C]	177.77	627.77	162.77	862.27	627.77	227.7	157.77	227.77	877.58	427.7	427.77	227.77
Shell operating temperature [°C]	150	600	135	834.5	600	200	130	200	849.8	400	400	200
Tube length extended [meter]	6.096											
Tube pitch [meter]	0.031											
Number of tube passes	1											
Number of shell passes	1											

Table 14: Detail design of box furnaces.

Equipment	HT1	HT3	HT6	HT5
Duty [cal/sec]	1398941.13	46848.39	104003.59	282798.72
Standard gas flow rate [L/min]	888.39	2002.88	18.63	1017.26
Process type	LIQ			
Design gauge pressure [bar]	9.710			
Design temperature [°C]	827.77	627.7	277.7	577.77

Table 15: Detail design of jacketed horizontal drums.

Equipment	MIDTRX	HITRX
Liquid volume [l]	5854.71	1801.44
Vessel diameter [meter]	1.3716	0.9144
Vessel tangent to tangent length [meter]	3.9624	2.7432
Design gauge pressure [bar]	9.710	9.710
Design temperature [°C]	862.27	1027.77
Operating temperature [°C]	834.5	1000

Table 16: Detail designing of Reactor HITRX.

Parameters	HITRX
Operating temperature range (°C)	850-1000
Pressure (bar)	9
Mass flow $_{in}$ (SO_3)	2056.11
Mass flow $_{out}$ (SO_3)	381.25

Table 17: Design spec block use for SO_3 conversion.

Design Spec	Status	Error	Tolerance	Error Tolerance	Variable value
SO_3-CONV	Converged	5.04E-06	0.001	0.00504	0.182

The characteristics selected for the reactor design are; CSTR reactor (but no stirring), homogenous reactants, and 1st order kinematics. Table 16 shows the configuration of reactor HITRX [24-30].

Input=Output +Disappearance by reaction + Acculation (10)

For calculating the reactor volume, the parameters are F_{AO} is 2056.11 kmol/h, F_A is 381.25 kmol/h, Vol_{in} is 265.99 m^3/h, X_A is 0.185425828, K (kinetic factor) is 30.55, C_A and $-r_A$. By applying all calculations, reactor volume is found to be 1614.384 L. The reactor volume matches the HITRX Aspen Model.

Convergence criteria

Convergence in Aspen Plus is obtained through solvers. They work behind the Aspen Plus model solution. By generating the result, they will make sure that the result is possible through successful iterations adjustment of tolerance is another way to achieve convergence but with more errors. Table 17 shows the design spec block, which helped in convergence.

By using the convergence monitor in Aspen Plus®, Figs. 5 and 6 are made. They have shown a comparison between convergence index and iteration based on design spec and overall maximum error.

Model validation

This process can be a massive benefactor for small industries regarding energy production. The standard equipment and utilities like turbines, compressors, heat exchangers, and flow distributors have a perfect validation for scale-up and down is shown in Table 18. The essential equipment of the process, the electrolyzer, has some

Table 18: Model comparison.

Model Compare	Nel Hydrogen M2000	Current Electrolyzer
Net production rate (L/min)	33333.33	398.48
Net production rate (kg/day)	4,319	943.08
Average power consumption (kWh/Nm³)	4.5	28.33
Delivery pressure (bar)	30	21.5
Ambient temperature (°C)	40	50

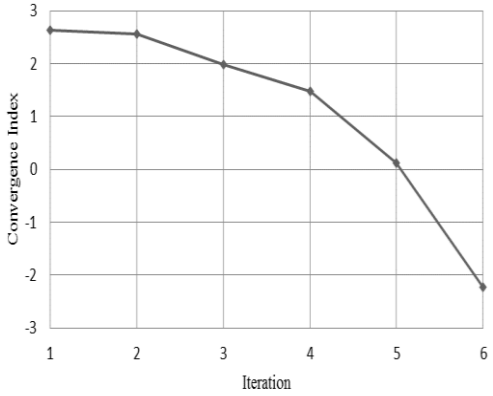

Fig. 5: Overall maximum errors.

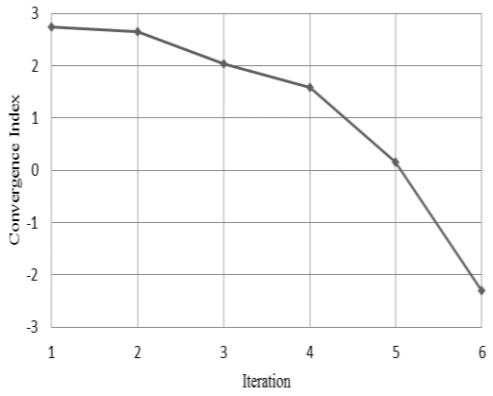

Fig. 6: Design spec block.

problems with model validation, as initially, hydrogen production was 10,000 kg/hrs (approx.). Still, after this research on different electrolyzers, it was found out that normal electrolyzers produce a max of 20 kg/hr. After changing the design and the overall flow, this process generates 39 kg/hr. The model equipment used for this design is M-series by Nel hydrogen [20, 24, 30-35].

CONCLUSIONS

This research has made an effective process and adopted a low budget and efficient method of H_2 production by solar thermochemical water splitting process. This process is in which S and NH_3 are used as thermo chemicals. The long-lasting sustainability of the whole thermo-electrical process can be explained by five thousand Plus hours of operation. A particular type of PEM (proton exchange membrane) is used in ELECTLYZ that increases efficiency. These PEM (proton exchange membranes) are sustainable even after running this process @413K. Aspen Plus® results prove the approach's feasibility; NH_3 and SO_3 evolved separately without separating the complex membrane. The SO_3 degradation is a proven method. For this process, Aspen Plus® is used to design the plant efficiently. Because of the variation of the phase change method of solar energy, NaCl was installed to allow continuous operation of plant @1063K. A Rankin cycle was outlined to regain excess energy to produce electricity more efficiently. The total pressure of the plant was 9 bar which can be changed to improve the effectiveness and power regaining ability of the plant. The solar sulfur ammonia cycle for the production of hydrogen gas is an effective process because, in this process, zero greenhouse gases are produced. This plant is comparatively operated at low temperature and operated @1073K.All the waste heat is utilized to produce electricity. This plant mainly needs low-cost equipment, and due to this reason, it can quickly pay back the loan. For future improvements, recommendations are; the most expensive equipment of the plant is the ELECTLYZ, which represents at least 38% of the total cost. It reduces the price, and it is better to use a low-cost membrane for the electrolyzer. The fundamental thing is solar energy to run the plant, but the method of its extraction is very much costly and difficult because a wide area is needed for this. So need a more modified way to extract solar energy for the solar thermochemical to run smoothly at a low cost.

Declaration of Competing Interest

With the submission, all authors confirm no conflict of interest and ensure that this article has not been previously published and is not under consideration by another Journal.

Acknowledgments

The authors would like to acknowledge the Department of Chemical Engineering and Department of Polymer and Petrochemical Engineering, NED University of Engineering & Technology, Karachi, Pakistan, for supporting this research work.

Abbreviation

LOTRX = Low Temperature Reactor, MIDTRX = Mid Temperature Reactor, HITRX = High Temperature Reactor, ABSRX = Absorber, ELECTLYZ = Electrolyzer

Received : Dec. 30, 2021 ; Accepted : Apr. 18, 2022

REFERENCES

[1] Budama V.K., Johnson N.G., McDaniel A., Ermanoski I., Stechel E.B., Thermodynamic Development and Design of a Concentrating Solar Thermochemical Water-Splitting Process for Co-Production Of Hydrogen and Electricity, *Int. J. Hydrogen Energy*, **43**: 17574-17587 (2018).

[2] Sadeghi S., Ghandehariun S., Thermodynamic Analysis and Optimization of an Integrated Solar Thermochemical Hydrogen Production System, *Int. J. Hydrogen Energy*, **45**: 28426-28436 (2020).

[3] Liu T., Liu Q., Lei J., Sui J., A new Solar Hybrid Clean Fuel-Fired Distributed Energy System with Solar Thermochemical Conversion, *J. Cleaner Prod.*, **213**: 1011-1023 (2019).

[4] Boretti A., Nayfeh J., Al-Maaitah A., Hydrogen Production by Solar Thermochemical Water-Splitting Cycle via a Beam Down Concentrator, *Front. Energy Res.*, **9**: 1-5 (2021).

[5] Siegrist S., von Storch H., Roeb M., Sattler C., Moving Brick Receiver–Reactor: A Solar Thermochemical Reactor and Process Design With a Solid–Solid Heat Exchanger and On-Demand Production of Hydrogen and/or Carbon Monoxide, *J. Sol. Energy Eng.*, **141**: 1-12 (2019).

[6] Boretti A., Technology Readiness Level of Solar Thermochemical Splitting Cycles, *ACS Energy Lett.*, **6**: 1170-1174 (2021).

[7] Chen J., Xu W., Zuo H., Wu X., J. E, Wang T., Zhang F., Lu N., System Development and Environmental Performance Analysis of a Solar-Driven Supercritical Water Gasification Pilot Plant for Hydrogen Production Using Life Cycle Assessment Approach, *Energy Convers. Manage.*, **184**: 60-73 (2019).

[8] Ahangar N., Mehrpooya M., Thermaly Integrated Five-Step ZnSI Thermochemical Cycle Hydrogen Production Process Using Solar Energy, *Energy Convers. Manage.*, **222**: 1-21 (2020).

[9] Moser M., Pecchi M., Fend T., Techno-Economic Assessment of Solar Hydrogen Production by Means of Thermo-Chemical Cycles, *Energies*, **12**: 1-17 (2019).

[10] Brendelberger S., Rosenstiel A., Lopez-Roman A., Prieto C., Sattler C., Performance Analysis of Operational Strategies for Monolithic Receiver-Reactor Arrays in Solar Thermochemical Hydrogen Production Plants, *Int. J. Hydrogen Energy*, **45**: 26104-26116 (2020).

[11] T. Kodama, S. Bellan, N. Gokon, H.S. Cho, Particle Reactors for Solar Thermochemical Processes, *Sol. Energy*, **156**: 113-132 (2017).

[12] Sayyaadi H., Saeedi Boroujeni M., Conceptual Design, Process Integration, and Optimization of a Solar CuCl Thermochemical Hydrogen Production Plant, *Int. J. Hydrogen Energy*, **42**: 2771-2789 (2017).

[13] Liu T., Bai Z., Zheng Z., Liu Q., Lei J., Sui J., Jin H., 100 kWe Power Generation Pilot Plant with a Solar Thermochemical Process: Design, Modeling, Construction, and Testing, *Appl. Energy*, **251**: 1-11 (2019).

[14] Sadeghi S., Ghandehariun S., Naterer G.F., Exergoeconomic and Multi-Objective Optimization of a Solar Thermochemical Hydrogen Production Plant with Heat Recovery, *Energy Convers. Manage.*, **225**: 1-16 (2020).

[15] Zheng Z., Liu T., Liu Q., Lei J., Fang J., A Distributed Energy System Integrating SOFC-MGT with Mid-and-Low Temperature Solar Thermochemical Hydrogen Fuel Production, *Int. J. Hydrogen Energy*, **46**: 19846-19860 (2021).

[16] Xing H., Yuan Y., Huiyuan Z., Yong S., Bingxi L., Heping T., Solar Thermochemical Hydrogen Production Using Metallic Oxides, *Energy Sources A: Recovery Util. Environ. Eff.*, **39**: 257-263 (2017).

[17] Schrader A.J., De Dominicis G., Schieber G.L., Loutzenhiser P.G., Solar Electricity *via* an Air Brayton Cycle with an Integrated Two-Step Thermochemical Cycle For Heat Storage Based on Co_3O_4/CoO Redox Reactions III: Solar Thermochemical Reactor Design and Modeling, *Sol. Energy*, **150**: 584-595 (2017).

[18] Hoskins A.L., Millican S.L., Czernik C.E., Alshankiti I., Netter J.C., Wendelin T.J., Musgrave C.B., Weimer A.W., Continuous on-sun Solar Thermochemical Hydrogen Production via an Isothermal Redox Cycle, *Appl. Energy*, **249**: 368-376 (2019).

[19] Schrader A.J., Schieber G.L., Ambrosini A., Loutzenhiser P.G., Experimental Demonstration of a 5 Kwth Granular-Flow Reactor for Solar Thermochemical Energy Storage with Aluminum-Doped Calcium Manganite Particles, *Appl. Therm. Eng.*, **173**: 1-8 (2020).

[20] Ma Z., Li M.-J., He Y.-L., Zhang K.M., Effects of Partly-Filled Encapsulated Phase Change Material on the Performance Enhancement of Solar Thermochemical Reactor, *J. Cleaner Prod.*, **279**: 1-17 (2021).

[21] Cumpston J., Herding R., Lechtenberg F., Offermanns C., Thebelt A., Roh K., Design of 24/7 Continuous Hydrogen Production System Employing The Solar-Powered Thermochemical S–I Cycle, *Int. J. Hydrogen Energy*, **45**: 24383-24396 (2020).

[22] Ishaq H., Dincer I., Design and Performance Evaluation of a New Biomass and Solar Based Combined System with Thermochemical Hydrogen Production, *Energy Convers. Manage.*, **196**: 395-409 (2019).

[23] Mehrpooya M., Tabatabaei S.H., Pourfayaz F., Ghorbani B., High-Temperature Hydrogen Production by Solar Thermochemical Reactors, Metal Interfaces, and Nanofluid Cooling, *J. Therm. Anal. Calorim.*, **140**: 1-23 (2020).

[24] Bayon A., Calle A.d.l., Effect of Plant Location on the Annual Performance of a Hydrogen Production Plant Based on CeO_2 Thermochemical Cycle, *AIP Conf. Proc.*, **2126**: 1-9 (2019).

[25] Villafán-Vidales H.I., Arancibia-Bulnes C.A., Riveros-Rosas D., Romero-Paredes H., Estrada C.A., An Overview of the Solar Thermochemical Processes for Hydrogen and Syngas Production: Reactors, and Facilities, *Renew. Sustain. Energy Rev.*, **75**: 894-908 (2017).

[26] Norouzi N., Fani M., Talebi S., Exergetic Design and Analysis of a Nuclear SMR Reactor Tetrageneration (Combined Water, Heat, Power, and Chemicals) with Designed PCM Energy Storage and a CO_2 Gas Turbine Inner Cycle, *Nucl. Eng. Technol.*, **53**: 677-687 (2021).

[27] Fani M., Norouzi N., Ramezani M., Energy, Exergy, and Exergoeconomic Analysis of Solar Thermal Power Plant Hybrid with Designed PCM Storage, *Int. J. Air-Cond., Refrig.*, **28**: 1-7 (2020).

[28] Norouzi N., 4E Analysis of a Fuel Cell and Gas Turbine Hybrid Energy System, *Biointerface. Res. Appl. Chem.*, **11**: 7568-7579 (2021).

[29] Norouzi N., Talebi S., Fani M., Hossein K., Heavy Oil Thermal Conversion and Refinement to the Green Petroleum: A Petrochemical Refinement Plant Using the Sustainable Formic Acid for the Process, *Biointerface. Res. Appl. Chem.*, **10**: 6088-6100 (2020).

[30] Norouzi N., Morteza H., Talebi S., Fani M., A 4E Analysis of Renewable Formic Acid Synthesis from the Electrochemical Reduction of Carbon Dioxide and Water: Studying Impacts of the Anolyte Material on the Performance of the Process, *J. Cleaner Prod.*, **293**: 1-26 (2021).

[31] Norouzi N., Talebi S., Fani M., Hossein K., Exergy and Exergoeconomic Analysis of Hydrogen and Power Cogeneration Using an HTR Plant, *Nucl. Eng. Technol.*, **53**: 2753-2760 (2021).

[32] Norouzi N., Assessment of Technological Path of Hydrogen Energy Industry Development: A Review, *Iran. J. Energy Environ.*, **12**: 273-284 (2021).

[33] Norouzi N., Fani M., Energy and Exergy Analysis and Selection of the Appropriate Operating Fluid for a Combined Power and Hydrogen Production System Using a Geothermal Fueled ORC and a PEM Electrolyzer, *Iran. J. Chem. Chem. Eng. (IJCCE)*, I**41(5):** 1786-1803 (2022).

[34] Norouzi N., Fani M., Hydrogen Industry: A Technical, Economic, and Market Analysis Overview, *Online J. Chem.*, **1**: 59-84 (2021).

[35] Norouzi N., Talebi S., Exergy, Economical and Environmental Analysis of a Natural gas Direct Chemical Looping Carbon Capture and Formic acid-Based Hydrogen Storage System, *Iran. J. Chem. Chem. Eng. (IJCCE)*, **41(4):** 1436-1457 (2022).